MESQUITE: PETROGRAPHY, ALUMINUM-26 CHRONOMETRY, AND BE-B SYSTEMATICS OF AN UNUSUALLY LARGE MELILITE-RICH CAI FROM THE NORTHWEST AFRICA (NWA) 7892 CO3.0 CHONDRITE. A. T. Hertwig[1], E. T. Dunham[2], M.-C. Liu[1], and M. Wadhwa[2] [1]Department of Earth, Planetary, and Space Sciences, University of California-Los Angeles, Los Angeles, CA 90095, USA (hertwig@ucla.edu), [2]Center for Meteorite Studies, School of Earth and Space Exploration, Arizona State University, Tempe, AZ 85287, USA.

Introduction: Calcium-aluminum-rich inclusions (CAIs) are one of the oldest solids in the Solar System and therefore record information about processes in the solar nebula. For instance, the Be-B systematics of CAIs records information about the irradiation environment [e.g., 1, 2] because short-lived ^{10}Be (decays to ^{10}B) is exclusively formed by energetic particle spallation [e.g., 3]. On the other hand, the Al-Mg systematics in CAIs provides a relative timeframe for condensation or heating events during the Solar System's early evolution.

While most chondrite groups contain them, CAIs differ between groups in their size distribution, abundance, and relative proportion [e.g., 4]. Most isotopic investigations, including studies of Al-Mg and Be-B systematics [e.g., 2, 5], have been focused on CAIs from CV3 chondrites due to large inclusion sizes and high abundances of CAIs in this chondrite group. Just a few studies have focused on CAIs from other groups, e.g., CM or CO chondrites [6–8].

CAIs from CO chondrites make up ~1 vol.% of the meteorite and are usually small in size (up to 500 µm) [4, 8]; melilite-rich, spinel-pyroxene, and hibonite-hercynite types dominate [8]. A previous study demonstrates that some CAIs from CO chondrites show evidence for having incorporated ^{26}Al, with most CAIs being characterized by an initial ^{26}Al/^{27}Al ratio of ~5×10^{-5} [8], consistent with the canonical value of 5.2×10^{-5} within errors [5]. Lower ^{26}Al/^{27}Al have also been reported for other CO3 chondrite CAIs [6]. The incorporation of short-lived ^{10}Be in CO CAIs has been demonstrated so far for one mineralogically pristine inclusion in Dominion Range (DOM) 08006; it records (^{10}Be/^{9}Be)=$(15.0\pm0.7)\times10^{-4}$ [9]. This falls within the range of inferred initial ^{10}Be/^{9}Be in CV3 CAIs [10, refs therein]. However, more CO3 CAIs need to be measured to understand the distribution of ^{10}Be/^{9}Be in CAIs of this chondrite group.

Here we report the petrological characterization of CAI Mesquite from the CO3 Northwest Africa (NWA) 7892 and its initial ^{26}Al/^{27}Al and ^{10}Be/^{9}Be ratios to better understand this CAI's formation history.

Methods: The thin section containing the Mesquite CAI was imaged by standard electron microscopic techniques (SE, BSE) using the JEOL JXA-8530F at ASU. Mineral chemistries of melilite, hibonite, and spinel were determined with the JEOL JXA-8200 Superprobe at UCLA.

Be-B and Al-Mg systematics were analyzed on the UCLA CAMECA ims-1290 ion microprobe using an $^{16}O^-$ primary ion beam generated by the Hyperion-II plasma ion source. Primary beam intensities were 7 nA and 10 nA (< 4 µm beam size) for Be-B analyses. The Be-B systematics of melilite and hibonite were determined by following the method described in [9]. At the beginning of the analytical session, the relative sensitivity factor (RSF) affecting the ^{9}Be/^{11}B ratios of unknowns was determined by measuring the NBS614 glass standard which was also used for determining the instrumental mass fractionation affecting the ^{10}B/^{11}B ratios.

Primary beam intensities ranged from 1 to 15 nA (1-5 µm) for Al-Mg analyses. Al-Mg systematics of spinel and hibonite were measured in multi-collection mode using Faraday cups on the multi-collection array by following the method described in [11]. RSFs for accurate ^{27}Al/^{24}Mg ratios were obtained by measuring terrestrial standards whose ^{25}Mg/^{24}Mg and ^{26}Mg/^{24}Mg ratios are assumed to be those of [12]. We used an exponential fractionation law (β=0.5128) and express the excess of ^{26}Mg produced by the decay of ^{26}Al after correction for mass-dependent fractionation as Δ^{26}Mg* (‰). Isochrons were calculated using the Isoplot macro collection [13] (Model 1 fit).

Petrography and mineralogy: The CAI is about 5 × 3 mm and by far the largest object in the section (Fig. 1). Melilite is the most abundant mineral followed by hibonite, spinel, and perovskite. The inclusion has a

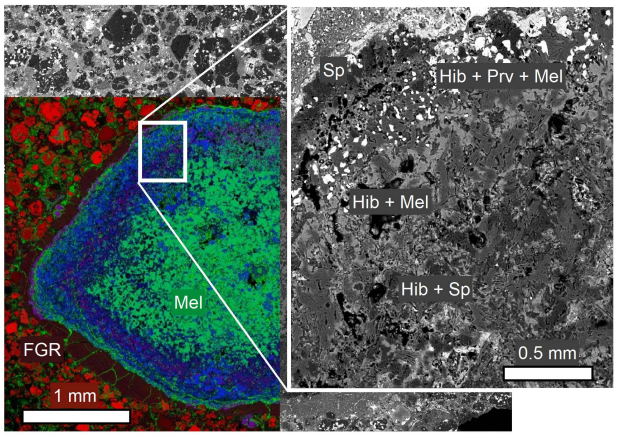

Fig. 1: Electron images showing texture of CAI Mesquite. Colors in EDS map - red: Mg, blue: Al, green: Ca; Hib: hibonite, Mel: melilite, Prv: perovskite, Sp: spinel; FGR: fine-grained rim.

compact, prismatic shape with rounded edges, is mineralogically zoned (concentric), and is surrounded by a fine-grained rim (FGR). The center zone is dominated by melilite, whose grain size is less than 200 μm, and enclaves of hibonite. Spinel or perovskite are absent. Layers of hibonite-spinel, hibonite-melilite, hibonite-perovskite-melilite, and spinel surround the center melilite; boundaries between layers are in general parallel to margins. The chemical composition of hibonite (MgO = 2.6±1.1 wt.%, 2SD, n=37) does not vary systematically from layer to layer; melilite seems to be slightly more Mg-rich in the center (Ak=3±4, 2SD, n=32) relative to the outer layer (Ak=1.3±1.0, 2SD, n=11). Secondary minerals identified by EDS measurements are calcite, which fills voids and fissures, and phyllosilicates.

Al-Mg and Be-B systematics: Hibonite and spinel show resolvable excess ^{26}Mg, with Δ^{26}Mg* values of up to 16‰ (for hibonite). The slope of the resulting isochron translates to an initial ^{26}Al/^{27}Al ratio of $(5.0 \pm 0.2) \times 10^{-5}$ (MSWD = 4.3, 95%-conf.). The δ^{25}Mg values of hibonite (~ −6‰, n=10) and spinel (~ −3‰, n=2) in the hibonite-spinel layer are negatively fractionated; spinel in the outermost layer show positively fractionated δ^{25}Mg values (~ +3‰, n=1). We note that these results are of preliminary nature due the small number of measurements. Melilite and hibonite were analyzed for Be-B and show evidence for having incorporated live ^{10}Be. Isochron regression yields ^{10}Be/^{9}Be=(10.0±6.6)×10^{-4} and ^{10}B/^{11}B=0.248±0.009 (MSWD=0.8, 2σ errors).

Discussion: With a maximum length of 5 mm, Mesquite is larger than most CAIs in CO chondrites [4, 8]. Considering the inclusion size, shape, and mineralogy, Mesquite could be best described as a compact Type A (CTA) inclusion; however, melilite does not appear blocky and grains are smaller than those in a typical CTA [14]. Another distinct feature of this CAI is the concentric layering that resembles Wark-Lovering rims [15].

The initial ^{27}Al/^{26}Al ratio of $(5.0 \pm 0.2) \times 10^{-5}$ is indistinguishable from the canonical value [5]. Interestingly, all hibonite grains and spinel in the hibonite-spinel zone are negatively fractionated which might point to a condensation origin. On the contrary, spinel in the outermost zone has a positive δ^{25}Mg value, implying that the rim of the inclusion could have been once molten and undergone evaporation. We will perform more measurements on the rim phases to confirm this.

The initial ^{10}Be/^{9}Be ratio (10.0±6.6)×10^{-4} for CAI Mesquite is within the range of previously measured CAIs [10, refs therein]. This implies that most CAIs were irradiated with a similar dose of energetic particles.

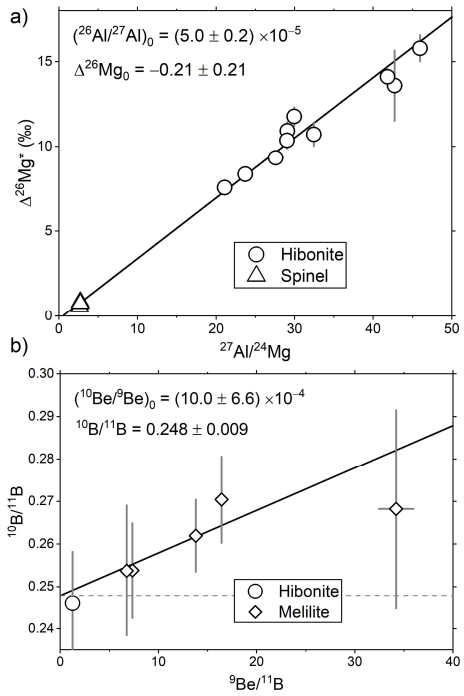

Fig. 2: (a) Al-Mg and (b) Be-B systematics of Mesquite CAI. Data point errors are 2σ; uncertainty in the initial ^{27}Al/^{26}Al ratio is 95%-confidence interval; 2σ for ^{10}Be/^{9}Be.

The size and texture set Mesquite apart from other CAIs from CO chondrites and warrant further studies of oxygen isotope and trace element systematics. The initial ^{10}Be and ^{26}Al results reported here indicate that this CAI is isotopically similar to other CAIs. This strengthens arguments that ^{26}Al was introduced to the solar nebula by an external source while ^{10}Be was produced by energetic particle spallation of CAIs or their precursors in the solar nebula [e.g., 2].

References: [1] Chaussidon M. et al. (2006) *GCA*, 70, 224–245. [2] Liu M.-C. et al. (2010) *ApJ*, 719, L99-L103. [3] Fowler W. A. et al. (1961) *Am. J. Phys.,* 29, 393–403. [4] Scott E. R. D. and Krot A. N. (2007) *In: Treatise on Geochemistry, Vol. 1*, 1–72. [5] Jacobsen B. et al. (2008) *EPSL*., 272, 353–364. [6] Simon S. B. et al. (2019) *GCA*, 246, 109–122. [7] Liu M.-C. et al. (2012) *EPSL*, 327-328, 75–83. [8] Russell S. S. et al. (1998) *GCA*, 62, 689–714. [9] Dunham E. T. et al. (2018) *LPS XLIX*, #2402. [10] Liu M.-C. and Chaussidon M. (2018) *In: Boron isotopes*, 5, 273–289. [11] Liu M.-C. et al. (2017) *Int. J. Mass Spectrom.*, 424, 1–9. [12] Catanzaro E. J. et al. (1966) *J. Res. Natl. Bur. Stan., Sect. A*, 70A, 453. [13] Ludwig K. R. (2008) *Berkeley Geochronology Center, Special Pub.*, 4, 1–76. [14] Brearley A. J. and Jones R. H. (1998) *Rev. Mineral. Geochem.,* 36, 3-01 - 3-398. [15] Wark D. A. and Lovering J. F. (1977) *Proc. Lunar Sci. Conf. 8th*, 95–112.